Digital Signal Processing **12**, 329–346 (2002)
doi:10.1006/dspr.2002.0448

# Diversity Waveform Signal Processing for Delay–Doppler Measurement and Imaging

Mark R. Bell and Stephane Monrocq

School of Electrical and Computer Engineering, Purdue University, West Lafayette, Indiana 47907-1285

Bell, M. R., and Monrocq, S., Diversity Waveform Signal Processing for Delay–Doppler Measurement and Imaging, *Digital Signal Processing* **12** (2002) 329–346.

Coherent pulse–Doppler radar systems, whether used for synthetic aperture imaging or surveillance purposes, generally transmit a coherent pulse train made up of identical pulses. While these pulses may contain complex modulation—for example, linear FM chirps or frequency and phase coding—the fact remains that these pulses are usually identical. In this paper, we consider the potential advantages of pulse trains made up of pulses that are distinctly different from pulse-to-pulse. In particular, we investigate a signal processing algorithm that provides increased resolution and discrimination through delay–Doppler sidelobe suppression in the region surrounding the mainlobe of the delay–Doppler response.


*Key Words:* signal theory; time-frequency resolution; radar waveforms; ambiguity functions; coded waveforms.

## 1. INTRODUCTION

As radar matured as a sensing technology throughout the 1960–1980s, standard approaches to radar waveform design in pulse–Doppler radar systems became established. Many of these techniques—either explicitly or implicitly—were influenced by the signal processing and waveform generation technologies available at the time. As a result, the standard techniques adopted in pulse–Doppler radar were influenced by a combination of signal theory and technological constraints. Significant increases in computer processing power and the development of flexible programmable digital modulators have drastically changed the potential capabilities available for radar waveform design and processing, opening up the possibility of new levels of waveform adaptivity and adaptive processing for enhanced radar performance. In this work, we focus on developing these ideas in the context of pulse–Doppler radar.



1051-2004/02 $35.00

A cursory look at a simple matched filter radar illustrates a fundamental symmetry between the role of the transmitted waveform and the receiver matched filter. For the detection of point targets in additive white Gaussian noise, they are effectively equivalent (the receiver filter impulse response is the time-reversed conjugate of the transmitted waveform). Of course if the noise is not white, the matched filter is modified accordingly [1, Chap. 2], and if the targets are not point targets, both the waveform and the receiver filter are modified to maximize detection signal-to-noise ratio [2]. In some sense, both the transmitted waveform and the receiver signal processing play equally important—yet complementary—roles in radar performance. Recent years have seen increased activity in adaptive processing schemes for radar signal processing (e.g., space–time adaptive processing or STAP), but very little emphasis has been placed on waveform adaptation for enhanced performance. While on the one hand this is understandable—adaptive processing can be easily applied to measurements made by existing radars using fixed waveforms—adaptive processing alone will not yield optimal system performance. It is necessary to consider adaptation of the transmitted waveforms as well. In order to better understand the situation, we now look at how a pulse–Doppler radar makes measurements.

A radar system measures an environment of interest by illuminating it with coherent electromagnetic radiation. The illuminating field scattered by objects in the environment is collected by a receiver, which processes this scattered signal to determine the presence and scattering characteristics of the objects that scattered the illuminating signal. Two of the most important parameters characterizing the return from an individual point scatterer are the round-trip propagation delay time and the Doppler shift (a result of the Doppler effect, causing dilation or contraction of the received signal in time that is well approximated by a frequency shift for narrowband signals) imparted on the scattered waveform by radial motion of the scatterer with respect to the radar. In fact, the time delay and Doppler shift associated with the return from a scatterer are used as the primary coordinates for characterizing the scattered return in a pulse–Doppler radar processor.

A radar or other pulse–echo delay–Doppler measurement system can be viewed as an imaging system that forms a delay–Doppler image of the illuminated environment. We can think of the individual delays and Doppler shifts associated with individual scatterers as specifying points in a two-dimensional image with coordinates of delay $\tau$ and Doppler frequency shift $\nu$. When the received signal is processed by a matched filter matched to a replica of the transmitted waveform delayed by $\tau$ and shifted in frequency by $\nu$, the resulting measurement problem is equivalent to imaging the reflectivity of the illuminated environment using an aperture that is a function of the illuminating waveform [3; 4, p. 58]. In the narrowband case—which we assume throughout this paper—the point-spread function of the aperture is determined by the *ambiguity function* of the transmitted waveform.

Viewing delay–Doppler radar as an imaging system, it becomes clear that its ability to distinguish or discriminate between scatterers in delay and Doppler

is determined by its convolution kernel or point-spread function. We have some control in selecting this kernel, since it is the ambiguity function of the waveform we choose to transmit. However, some fairly strong constraints on the mathematical form of the ambiguity function prohibit us from obtaining the ideal imaging kernel—a delta function located at the origin of the $(\tau, \nu)$-plane. Hence it may not be possible to obtain the desired discrimination capability using a single pulse–echo measurement made with a single pulse waveform.

Viewing a radar system as a delay–Doppler imaging system that is the mathematical analog of an optical imaging system suggests a way around the delay–Doppler discrimination limitations of a single waveform measurement. In optical imaging and image processing, a number of investigators have considered the problem of constructing a high-resolution image using a number of low resolution imaging systems having sufficiently different point-spread functions [5–7]. The analogy between pulse–echo delay–Doppler measurements and optical imaging suggests that one way around this problem is to make multiple pulse–echo measurements using waveforms having sufficiently different ambiguity functions and then process and combine the individual waveform returns to form an enhanced discrimination delay–Doppler image. Such a waveform-diverse measurement technique would allow for increased capability to spatially discriminate among scatterers in radar imaging (where one coordinate is derived from delay and the other from Doppler shift). This is exactly the point of view we developed in [3].

For diversity waveform measurement to become a useful radar measurement tool, the diversity measurements would most likely need to be taken sequentially in time. The primary reason for this is economic—the cost of using parallel sensing systems becomes prohibitive. However, because we assume targets have nonzero Doppler (they are in motion), the target environment is changing from one sequential diversity measurement to the next. Straightforward application of the model considered in [3] would result in smeared or defocused images resulting from target motion from pulse-to-pulse. Even motions small relative to a range (delay)-resolution cell can result in a significant change in the phase of the scattered return. Of course it is exactly this coherent phase change with time through which the Doppler effect exhibits itself as a frequency shift for narrowband signals. Our approach to dealing with this comes directly from the standard pulse–Doppler processor architecture.

In this paper, we investigate a number of important issues relating to signal processing for waveform-diverse pulse–Doppler radar measurement. In Section 2, we discuss the fundamental measurement model and idea upon which resolution enhancement using diversity waveforms is based. In Section 3, we briefly review the results that have been obtained in the area of waveform-diverse pulse–Doppler measurement and discuss waveform design results for the idealized pulse–Doppler measurement model. In Section 4, we discuss the shortcomings of the idealized model as an accurate model of the pulse–Doppler measurement process, and we describe one approach to signal processing to overcome these shortcomings. We show simulation results applying this signal processing algorithm to diversity-waveform pulse–Doppler measurements and

show its performance in imaging closely spaced targets when compared to single waveform pulse–Doppler radar using standard pulse–Doppler processing techniques. Finally, in Section 5, we discuss the implications of these techniques for practical radar measurement

## 2. THE DIVERSITY-WAVEFORM MEASUREMENT MODEL

We now consider how a pulse–echo delay–Doppler measurement can be viewed as an imaging problem. Let $s(t)$ be the baseband analytic signal transmitted by the radar system. After being demodulated down to baseband, the received signal due to a scatterer with round trip delay $\tau_0$ and Doppler frequency shift $\nu_0$ is

$$r(t) = s(t - \tau_0)e^{j2\pi\nu_0 t}e^{j\phi},$$

where $e^{j\phi}$ is the phase shift in the received carrier due to the propagation delay $\tau_0$; hence $\phi = 2\pi f_0\tau_0$. If we process this signal with a matched filter

$$h_{\tau,\nu}(t) = s^*(T - t + \tau)e^{-j2\pi\nu(T-t)}$$

matched to the signal

$$q(t) = s(t - \tau)e^{j2\pi\nu t},$$

and designed to maximize the signal output at time $T$, the matched filter output at time $T$ is given by

$$\mathcal{O}_T(\tau, \nu) = e^{-j\phi}\chi_s(\tau - \tau_0, \nu - \nu_0). \tag{1}$$

Here $\chi_s(\tau, \nu)$ is the *ambiguity function* of $s(t)$ given by

$$\chi_s(\tau, \nu) = \int_{-\infty}^{\infty} s(t)s^*(t - \tau)\exp\{-i2\pi\nu t\}\,dt. \tag{2}$$

Because $h_{\tau,\nu}(t)$ is a linear time-invariant filter, by linearity, if $\mu(\tau, \nu)$ describes a continuous scattering density, the response of the matched filter $h_{\tau,\nu}(t)$ to this scattering density is

$$\mathcal{O}_T(\tau, \nu) = \int_{-\infty}^{\infty}\int_{-\infty}^{\infty} \gamma(t, v)\chi_s(\tau - t, \nu - v)\,dt\,dv, \tag{3}$$

where $\gamma(\tau, \nu) = \mu(\tau, \nu)e^{-j2\pi f_0\tau}$. This is the two-dimensional convolution of $\gamma(\tau, \nu)$ with $\chi_s(\tau, \nu)$ and can be thought of as the image of $\gamma(\tau, \nu)$ obtained using an imaging aperture with point-spread function $\chi_s(\tau, \nu)$ [12, Chap. 4], as shown in Fig. 1.

The viewpoint of a radar acting as an imaging system making a delay–Doppler image through an aperture whose point-spread function $\chi_s(\tau, \nu)$ is a function of the transmitted signal $s(t)$ is enlightening in terms of obtaining high resolution delay–Doppler images. We have some flexibility in selecting the

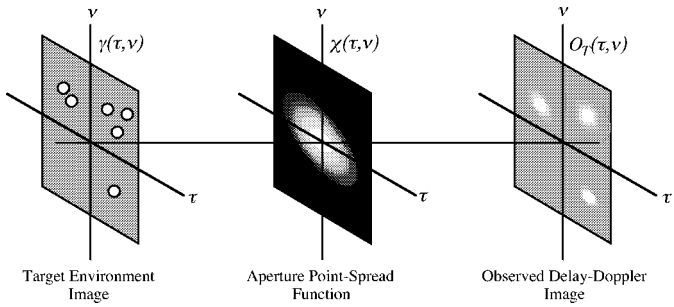


**FIG. 1.** Imaging interpretation of a delay–Doppler pulse–echo system. A waveform $s(t)$ with ambiguity function $\chi(\tau, \nu)$ gives rise to a delay–Doppler image $\mathcal{O}_T(\tau, \nu)$ that is the convolution of the ideal image $\gamma(\tau, \nu)$ with the point-spread function $\chi(\tau, \nu)$.

point-spread function $\chi_s(\tau, \nu)$ through selection of the waveform $s(t)$. There are, however, some fairly strong restrictions on the form of the ambiguity function $\chi_s(\tau, \nu)$. In particular, the volume under $|\chi_s(\tau, \nu)|^2$ is equal to $\chi_s(0, 0)^2$, the energy in $s(t)$ squared; $\chi(\tau, \nu)$ possesses a conjugate symmetry of the form $\chi(-\tau, -\nu) = e^{-i2\pi\nu\tau}\chi^*(\tau, \nu)$, which results in the symmetry relationship $|\chi(-\tau, -\nu)| = |\chi(\tau, \nu)|$ on its magnitude, and the restrictions on simultaneously high resolution in both delay and Doppler as imposed by the uncertainty principle, which states that the product of the mean-square duration $(\Delta t)^2$ and the mean-square bandwidth $(\Delta f)^2$ of the signal $s(t)$ must satisfy $(\Delta t)^2(\Delta f)^2 \geq 1/(4\pi)^2$ [13].

The problem of obtaining high resolution images from a number of lower resolution images obtained using optical imaging systems with differing aperture functions has been investigated by a number of investigators [5–7]. The application of this idea to radar imaging and measurement is more limited. The primary work in this area has been the work on chirp-tomographic radar by Bernfeld [8, 9] and others [14, 15], and limited previous work on diversity waveform techniques [3, 16, 17].

We now consider how resolution can be enhanced in both delay and Doppler using diversity waveform measurements. Consider an idealized situation in which a radar system is capable of operating simultaneously and independently on several independent channels. Each channel has its own transceiver and signal processor and is perfectly time-synchronized with the other channels. For the discussion of the idealized model of this section, we also assume there is no cross-talk between channels. Hence, at the output of each channel we have a two-dimensional image of the target environment. For a point target located at $(\tau_0, \nu_0)$, this can be formulated as

$$\begin{aligned}
\mathcal{O}_T^0(\tau, \nu) &= e^{j\phi}e^{-j2\pi(\nu-\nu_0)\tau_0}\chi_{s_0}(\tau - \tau_0, \nu - \nu_0) \\
\mathcal{O}_T^1(\tau, \nu) &= e^{j\phi}e^{-j2\pi(\nu-\nu_0)\tau_0}\chi_{s_1}(\tau - \tau_0, \nu - \nu_0) \\
&\vdots \\
\mathcal{O}_T^{N-1}(\tau, \nu) &= e^{j\phi}e^{-j2\pi(\nu-\nu_0)\tau_0}\chi_{s_{N-1}}(\tau - \tau_0, \nu - \nu_0),
\end{aligned} \tag{4}$$

where $\mathcal{O}_T^i(\tau, \nu)$ is the image obtained through the $i$th channel. Coherently summing the images gives a composite image

$$\mathcal{O}_T^C(\tau, \nu) = e^{j\phi} e^{-j2\pi(\nu-\nu_0)\tau_0} \sum_{i=0}^{N-1} \chi_{s_i}(\tau - \tau_0, \nu - \nu_0), \tag{5}$$

which can be thought of as an image of a point target generated by a new point-spread function

$$C(\tau, \nu) = \sum_{i=0}^{N-1} \chi_{s_i}(\tau, \nu). \tag{6}$$

This new point-spread function will be called the *composite ambiguity function* (CAF) or *combined ambiguity function*, as has been used in [17], to distinguish it from the ambiguity function of a single signal.

The *composite ambiguity function* described above gives the delay–Doppler response when a set of waveforms is used to make independent, noninterfering measurements of a target scene, with the individual returns being matched filtered and then coherently combined. As such, it provides the resulting delay–Doppler resolution characteristics of such a measurement. In [3], the use of the volume under the composite ambiguity surface was considered as a metric of the resolution and discrimination properties of a set of diversity waveforms, as it serves as a rough global measure of mainlobe width and sidelobe height and presence, but it does not address the distribution of sidelobes in delay and Doppler. In [3], it is shown that by selecting equal-energy orthogonal waveforms, this volume can be reduced by a factor of $N$ (i.e., the number of diversity waveforms used). In addition, as Hlawatsch [18, Chap. 8] points out, the composite ambiguity function is also a determining factor in the accuracy with which estimates of the delay and Doppler of a point target can be made using independent diversity waveform measurements in additive Gaussian white noise.

The key limitation in implementing this multiple waveform delay–Doppler imaging scheme is the ability to get several independent, noninterfering measurements of the target environment at a particular point in time, or else be able to estimate and compensate for scatterer motion if the measurements are made in time sequentially. This sequential approach and the signal processing techniques to achieve it will be discussed in Section 4.

## 3. DIVERSITY WAVEFORM DESIGN

The theorem on minimum ambiguity volume in [3, Theorem 1] provides a guide for selecting a set of signals for waveform-diverse multiple measurements. However, it does not provide a constructive method for doing so. A set of orthogonal signals may have a small composite ambiguity volume $V_{\text{amb}}^{(c)}$, but this ambiguity volume may be poorly distributed. To distribute the ambiguity so that the composite ambiguity surface has a sharp central peak and uniformly low

delay–Doppler sidelobes, appropriate modulation schemes are necessary. In [3], we investigated various phase and frequency coded modulation schemes that yield a composite ambiguity surface having these properties. We investigated the design of phase, frequency, and phase–frequency coded waveform sets having the desired properties. These coded waveforms were the focus of our investigation for three reasons:

1. They have constant amplitude and hence can be efficiently transmitted through the saturated power amplifiers found in typical radar systems.

2. They are easily generated using programmable vector modulators, resulting in waveforms that can be easily processed and adapted on-the-fly—a key requirement for adaptive waveform systems.

3. The pulses can be easily designed to have identical time-bandwidth products, a distinct advantage in designing and optimizing the receiver and processing, and one lacking from other diversity waveform schemes (e.g., Bernfeld's Chirp-tomographic radar [8, 9]).

These families of coded waveform sets have the form $\{s_0(t), s_1(t), \ldots, s_{K-1}(t)\}$, with members having the form

$$s_i(t) = \sum_{n=0}^{N-1} \psi_{i,n}(t - nT) \exp\{j2\pi d_{i,n} t/T\} \exp\{j\phi_{i,n}\}, \tag{7}$$

where each $s_i(t)$ consists of a sequence of $N$ baseband chips of length $T$, each having finite energy, and with each pulse in the sequence modulated by an integer frequency modulating index $d_{i,n}$ and a phase $\phi_{i,n}$ that can take on any real number value. The composite ambiguity function of the set is given by [3]

$$C(\tau, \nu) = \sum_{i=0}^{K-1} \sum_{n=0}^{N-1} \chi_{n,n}^{(i)}(\tau, \nu) + \sum_{i=0}^{K-1} \sum_{n=0}^{N-1} \sum_{\substack{m=0 \\ m \neq n}}^{N-1} e^{j(\phi_{i,n} - \phi_{i,m})} \chi_{n,m}^{(i)}(\tau, \nu). \tag{8}$$

Here

$$\chi_{\psi_n \psi_m}(\tau, \nu) = \int_{-\infty}^{\infty} \psi_n(t) \psi_m^*(t - \tau) e^{-j2\pi\nu t}\, dt,$$

and

$$\chi_{n,m}^{(i)}(\tau, \nu) = e^{j2\pi(d_{i,m}/T)\tau} e^{-j2\pi\nu nT} \chi_{\psi_{i,n}\psi_{i,m}}\left(\tau - nT + mT, \nu - \frac{d_{i,n}}{T} + \frac{d_{i,m}}{T}\right). \tag{9}$$

Note that we have decomposed the CAF into self-ambiguity and cross-ambiguity terms. Thus $C(\tau, \nu)$ is the superposition of $N$ auto-ambiguity functions (sidelobes) located at the origin and $N \times (N-1)$ cross-ambiguity functions located at $((n-m)T, (d_{i,n} - d_{i,m})/T)$ on the delay–Doppler plane. Furthermore, each of the cross-ambiguity functions carries a complex phase factor $e^{j(\phi_n - \phi_m)}$. By appropriately designing the waveforms in a waveform set such that the locations and phases of the cross-ambiguity terms in Eq. (8) result in significant cross-term

cancellation, we can design radar signal sets that provide substantial improvement in delay–Doppler discrimination. In [3], we designed a number of waveform sets with good resolution properties using this relationship, the results of Theorem 1 proved in [3], and known properties of good single waveforms with phase or frequency coding. The performance of the resulting waveform sets is very encouraging.

## 4. WAVEFORM-DIVERSE SIGNAL PROCESSING

The key limitation in implementing the multiple waveform delay–Doppler imaging scheme is the ability to get several independent noninterfering measurements of the target environment at a particular point in time or else be able to estimate and compensate for scatterer motion if the measurements are made in time sequentially. In situations where the target environment repeats periodically—for example in some radar astronomy or radar imaging problems where there is sufficient control of the radar–target trajectory (e.g., imaging a rotating satellite)—this would be straightforward. In most applications, this will not be the case. The presence of nonzero Doppler will cause successive phase shifts from pulse-to-pulse which will—at least partially, if not fully—corrupt the ideal sidelobe cancellation properties of the waveforms. In order to achieve sidelobe cancellation like that of the idealized situation, we would need to be able to separate out each of the received scatterer components from the received signal—a task effectively equivalent to resolving each of the scatterers—estimate the successive phase shift from pulse-to-pulse for each component, and compensate for these phase shifts in each scatterer component before coherently summing each pulse response for each scatter component. Instead, we consider a much simpler processor that approximates the ideal situation in the region around the mainlobe and provides significant—although less than ideal—sidelobe cancellation.

In order to propose a pulse–Doppler processor for a coherent pulse train made up of a diverse set of pulses, we look first at the standard pulse–Doppler processor for a coherent pulse train made up of identical pulses. The structure in this case suggests a pulse–Doppler processor for coherent diversity pulse trains.

Consider a complex baseband pulse train

$$s(t) = \sum_{j=1}^{M} a_j \, p(t - [j-1]\Delta)$$

made up of $M$ identical pulses of the form $p(t)$ repeated at intervals $\Delta$, where $\Delta$ is the pulse repetition interval of the pulse train and the amplitudes $a_j$ on each pulse are complex numbers which could correspond to intentional modulation by the transmitter or a modulation imparted on the pulse train during the propagation and measurement process—for example, a Doppler shift resulting from target motion. If we observe this waveform in the presence of additive

Gaussian noise with PSD $S_{nn}(f)$, it is easy to see that the matched filter $\tilde{H}_M(f)$ for the pulse train (with output sample time $T = M\Delta$) is

$$\tilde{H}_M(f) = \frac{\sum_{j=1}^{M} a_j^* P^*(f) e^{i2\pi f(j-1)\Delta}}{S_{nn}(f)} \cdot e^{-j2\pi f M\Delta} = H(f) \sum_{j=1}^{M} a_j^* e^{-i2\pi f(M-j)\Delta}, \quad (10)$$

where

$$H(f) = \frac{P^*(f)}{S_{nn}(f)} e^{-i2\pi f\Delta}$$

is the matched filter for a single pulse $p(t)$ yielding maximum signal-to-noise ratio when sampled at time $t_s = \Delta$. A block diagram of the pulse train matched filter is shown in Fig. 2a. Note that it is made up of a matched filter matched to the individual pulse shape; the output of this matched filter is sampled at the pulse repetition interval with an offset corresponding to the particular range (delay) cell of interest, and then the samples are multiplied by the conjugates of the complex modulation coefficients $a_j$ and summed so that they add coherently. Finally, at time $T = M\Delta$—after all pulses have been processed and summed—the output of the accumulator is sampled; this is the matched filter output for

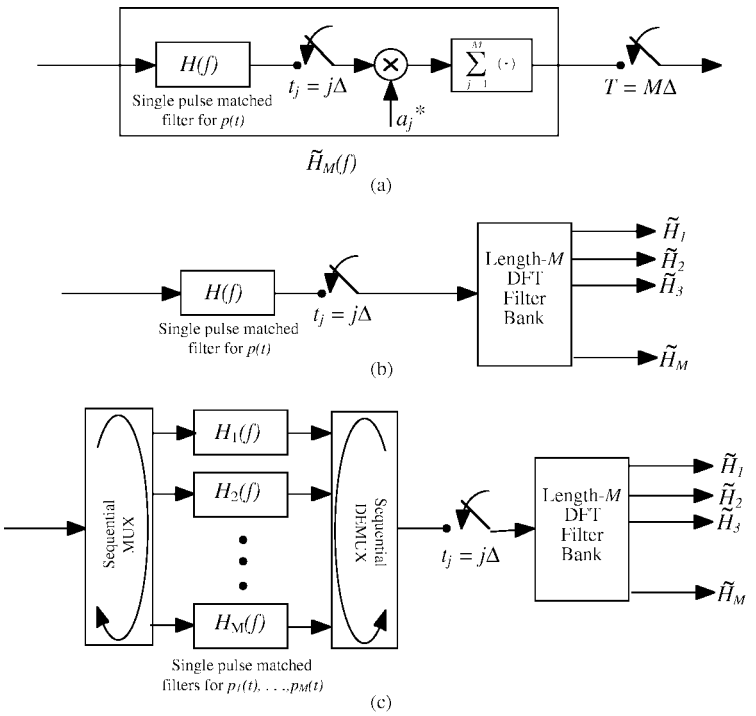


**FIG. 2.** Pulse–Doppler processors: (a) matched filter for a coherent pulse train of $M$ identical pulses having complex amplitude modulation $\{a_1, \ldots, a_M\}$; (b) pulse–Doppler processor for a coherent pulse train of $M$ identical pulses; (c) the proposed *multiplexed–waveform pulse–Doppler processor* for a coherent pulse train of $M$ different pulses.

the pulse train which can now be processed using a threshold test or more sophisticated detection processing (e.g., CFAR processing).

For narrowband signals (i.e., for $p(t)$ whose bandwidth is small compared to the radar carrier frequency), one of the most common forms of target induced modulation that is reflected in the $a_j$s is a Doppler frequency shift; for a Doppler frequency $f_D$, the coefficients $a_j$ will vary like

$$a_j = e^{i2\pi f_D j\Delta}.$$

The successive phase shift from pulse to pulse corresponds to a phasor rotation of $2\pi f_D\Delta$. Multiplication by $a_j^*$ performs a rotation in the opposite direction, resulting in the matched filter for the Doppler shifted pulse train if $f_D$ is known. In most pulse–Doppler radar systems, processing consists of taking the $M$ samples corresponding to the delay cell being processed and taking the $M$-point DFT of the sample sequence. This efficiently generates a bank of matched filters corresponding to $M$-matched filters for Doppler frequencies uniformly distributed over the $1/\Delta$-Hz unambiguous Doppler frequency interval. This processor is shown in Fig. 2b. This—perhaps most common—form of pulse–Doppler processor is what is most commonly found in pulse–Doppler radar systems. It is often a SAW device analog matched filter for the particular pulse used (although this can be implemented digitally) followed by digital processing corresponding to the DFT, perhaps with some enhanced form of processing (e.g., some form of windowing—perhaps adaptive—for enhanced clutter rejection in changing clutter environments or to achieve lower Doppler filter sidelobe levels). Note that the resulting filter band corresponds to a band of linear time-invariant filters.

When we now consider pulse–Doppler radar using coherent pulse trains made up of different pulses, $p_1(t), p_2(t), \ldots, p_M(t)$, a new form of processor needs to be used. In this case, we have that the waveform to be detected will be of the form

$$s(t) = \sum_{j=1}^{M} a_j p_j(t - (j-1)\Delta).$$

While we could derive the matched filter for this waveform, the ambiguity function of this waveform has $M(M-1)$ cross terms that can yield poor delay–Doppler performance. Actually, this would still correspond to matched filtering of a single waveform—the coherent pulse train made up of diversity pulses. Instead, why not switch the appropriate front end matched filters in and out in a synchronous matter, cycling through each of these pulse filters sequentially before sampling and computing the DFT? The resulting processor has a front end that looks very much like a polyphase filter bank, as can be seen in Fig. 2c. We call this processor the *multiplexed-waveform pulse–Doppler processor* (MWPDP). The interesting thing about this processor is that the sampled output for a target located in a range cell under test and having a Doppler frequency corresponding exactly to one of the frequencies in the Doppler filter bank is identical to that for the complete matched filter for the

**TABLE 1**

Coding Pattern for Joint Phase–Frequency Modulated Diversity Waveform Set Used in the Simulation

| $n$ | | 0 | 1 | 2 | 3 | 4 | 5 | 6 | 7 | 8 | 9 | 10 | 11 | 12 | 13 | 14 | 15 |
|---|---|---|---|---|---|---|---|---|---|---|---|---|---|---|---|---|---|
| $s_0(t)$ | $d_{0,n}$ | 1 | 4 | 3 | 7 | 7 | 2 | 0 | 6 | 6 | 0 | 2 | 7 | 7 | 3 | 4 | 1 |
| | $\phi_{0,n}$ | 0 | | | | 0 | | | | 0 | | | | 0 | | | |
| $s_1(t)$ | $d_{1,n}$ | 1 | 4 | 3 | 7 | 7 | 2 | 0 | 6 | 6 | 0 | 2 | 7 | 7 | 3 | 4 | 1 |
| | $\phi_{1,n}$ | 0 | | | | $2\pi/4$ | | | | $4\pi/4$ | | | | $6\pi/4$ | | | |
| $s_2(t)$ | $d_{2,n}$ | 1 | 4 | 3 | 7 | 7 | 2 | 0 | 6 | 6 | 0 | 2 | 7 | 7 | 3 | 4 | 1 |
| | $\phi_{2,n}$ | 0 | | | | $4\pi/4$ | | | | $8\pi/4$ | | | | $12\pi/4$ | | | |
| $s_3(t)$ | $d_{3,n}$ | 1 | 4 | 3 | 7 | 7 | 2 | 0 | 6 | 6 | 0 | 2 | 7 | 7 | 3 | 4 | 1 |
| | $\phi_{3,n}$ | 0 | | | | $6\pi/4$ | | | | $12\pi/4$ | | | | $18\pi/4$ | | | |
| $\psi_{i,n}(t) = P_T(t)$ for all $i$ and $n$ | | | | | | | | | | | | | | | | | |

diversity pulse train, but the overall delay–Doppler response does not have the cross terms present in the ambiguity function of the diversity pulse train. There is a significant cost, however. The resulting Doppler filter band is a time-varying Doppler filter bank.

In order to test the sidelobe cancellation characteristics of the MWPDP, we simulated its performance for a number of multiple target scenarios having targets close together in both delay and Doppler. We also simulated the performance of a standard pulse–Doppler processor processing a pulse train of identical pulses (the coded waveform $s_3(t)$ described in Table 1). In both cases, the pulse train used was made up of 24 pulses. The diversity waveform sets used for this simulation are the joint phase–frequency-coded waveforms described in [3, Table VIII, p. 1520]. Because there are only four waveforms in the set, we repeated the four waveforms six times each, with the pattern $s_0(t), s_1(t), s_2(t), s_3(t), s_0(t), s_1(t), s_2(t), s_3(t), \ldots, s_0(t), s_1(t), s_2(t), s_3(t)$.

The parameters of specification of these waveforms in terms of Eq. (7) are given in Table 1. The parameters of the simulated radar system are given in Table 2.

In order to characterize the MWPDP's sidelobe cancellation performance, we simulated its response to a number of different target scenarios. Here we will present the results of two of these—Scenario 1 having two targets and Scenario 2 having three targets. The target ranges and velocities for

**TABLE 2**

Simulated Radar System Waveform Parameters

| Parameter | Value |
|---|---|
| Carrier frequency | 1 GHz |
| Pulse repetition interval | 1 ms |
| Pulse duration (16 chips) | 12.6 $\mu$s |
| Pulses in pulse-train | 24 |
| Processor sampling rate | 80 MHz |

**TABLE 3**

Scenario 1 Target Ranges, Velocities, and Dopplers

| Parameter | Target 1 | Target 2 |
|---|---|---|
| Range (m) | 1000 | 840 |
| Velocity (m/s) | 400 | 400 |
| Doppler (Hz) | 2667 | 2667 |

Scenario 1 are given in Table 3, and those for Scenario 2 are given in Table 4. In order to focus on the ideal processor response, these simulations were carried out with very high signal-to-noise ratios (23.6 dB per pulse). Because of the close relationship between the standard pulse–Doppler processor and the multiplexed-waveform pulse–doppler processor, there is no reason to believe that lower signal-to-noise ratios in any way effect the relative ambiguity response.

The first thing we note in Fig. 3 when comparing the pulse–Doppler processor responses that when compared to the single waveform pulse–Doppler processor, the multiple waveform processor generates faint ghost images offset significantly in delay and Doppler from the true target locations (You have to look carefully to see these, as they are faint—about 15 dB below the true target response in this case). There also appears to be some cancellation of sidelobes around the true targets. In order to better investigate this, we will enlarge the response images about the true targets.

Figure 4 shows an enlarged view of the processor responses in the regions containing the targets. As can be seen from this image, significant sidelobe cancellation occurs, with sidelobe cancellation as large as 5 dB.

Similar results for Scenario 2 are presented in Figs. 5 and 6. Again, we see both the generation of weak ghost targets at a significant distance from the true targets by the multiple waveform diversity processor and the increased cancellation of sidelobes in the region around the true targets. Very similar results were obtained for several different target scenarios we tested.

## 5. DISCUSSION AND CONCLUSIONS

In this paper, we have considered the use of diversity waveform measurements in pulse–Doppler radar and simulated the performance of a simple suboptimal

**TABLE 4**

Scenario 2 Target Ranges, Velocities, and Dopplers

| Parameter | Target 1 | Target 2 | Target 3 |
|---|---|---|---|
| Range (m) | 1000 | 884 | 750 |
| Velocity (m/s) | 385 | 400 | 392 |
| Doppler (Hz) | 2567 | 2667 | 2613 |

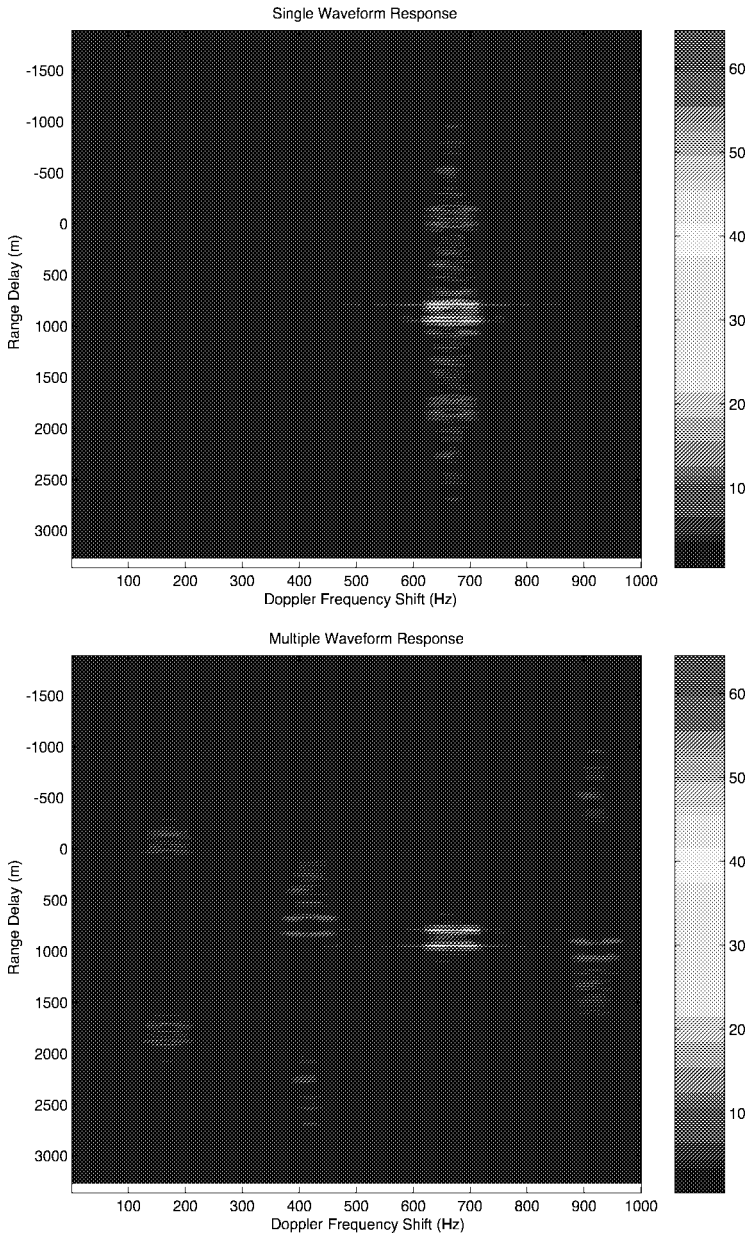


**FIG. 3.** Single and multiple waveform delay–Doppler response for two target scenario.

pulse–Doppler processor for use with diversity waveform sets. In looking at the resulting processor responses and comparing them, two specific results were noted:

1. The multiplexed-waveform pulse–Doppler processor generates weak ghost images of the real targets significantly displaced in delay and Doppler from the true targets.

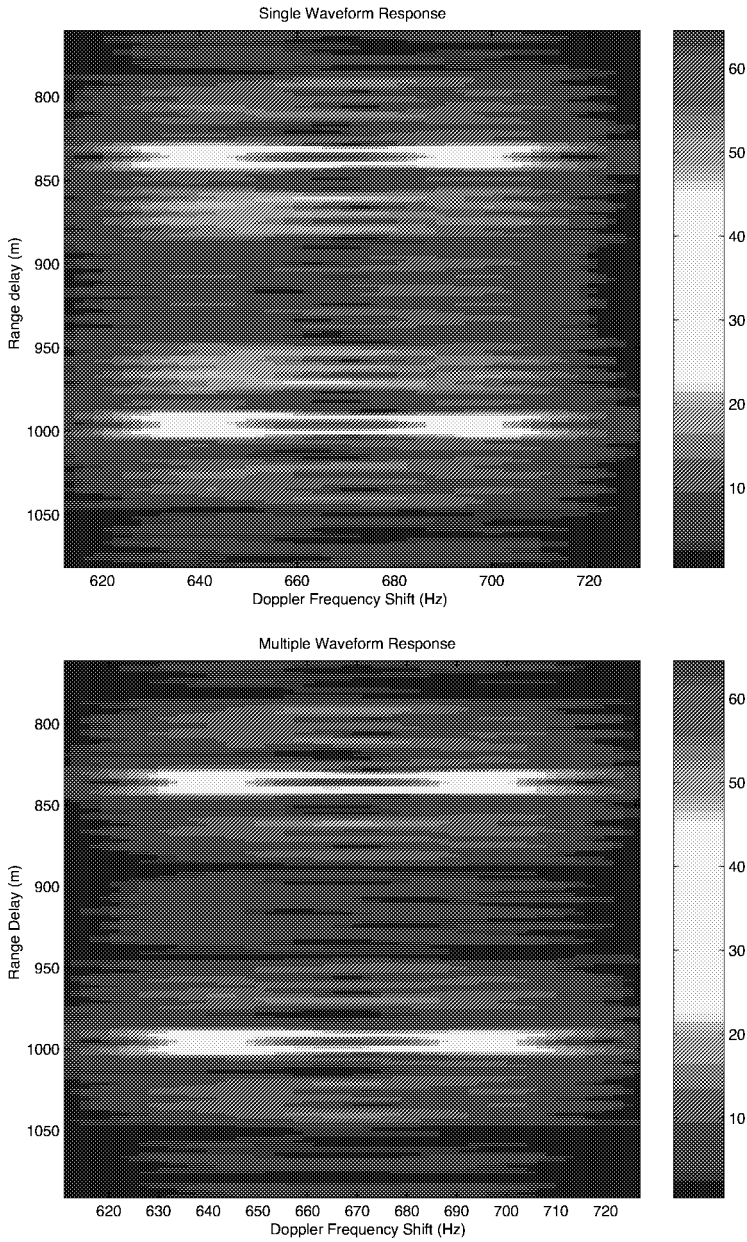


**FIG. 4.** Enlarged delay–Doppler response for two target scenario.

2. There is significant cancellation of delay–Doppler sidelobes and ambiguity volume—especially near the true target response mainlobe.

It is fairly clear that the first result can be considered bad news, while the second can be considered good news. False targets—even 15 dB or more down—can be a significant problem given that typical radar target reflectivities vary over a range of values much greater than this. Fortunately the false targets are

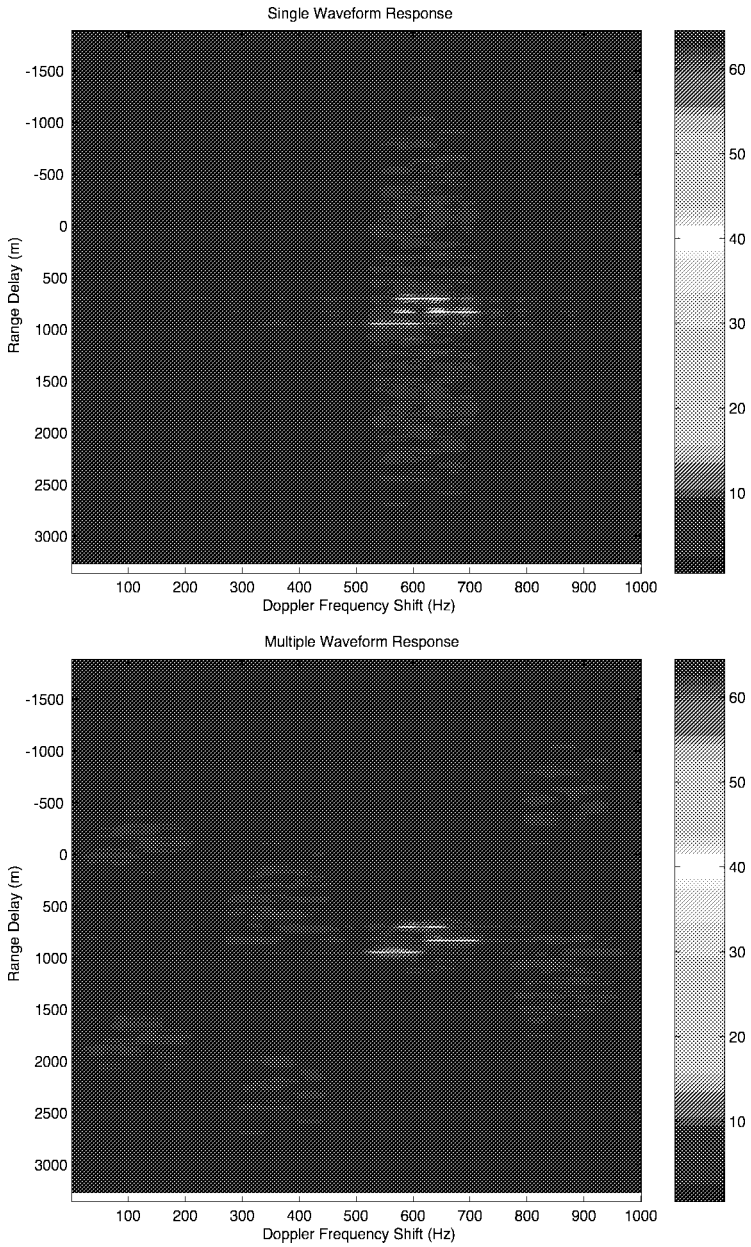


**FIG. 5.** Single and multiple waveform delay–Doppler response for three target scenario.

significantly displaced from the real targets, but they still present a significant problem from a radar using diversity waveforms and this type of processor. Of course the improved cancellation of sidelobes and ambiguity volume around the true targets is exactly what we wanted.

These two observations taken together suggest one possible form of an adaptive radar system that could make use of diversity waveforms and the multiplexed-waveform pulse–Doppler processor. The radar could initially use

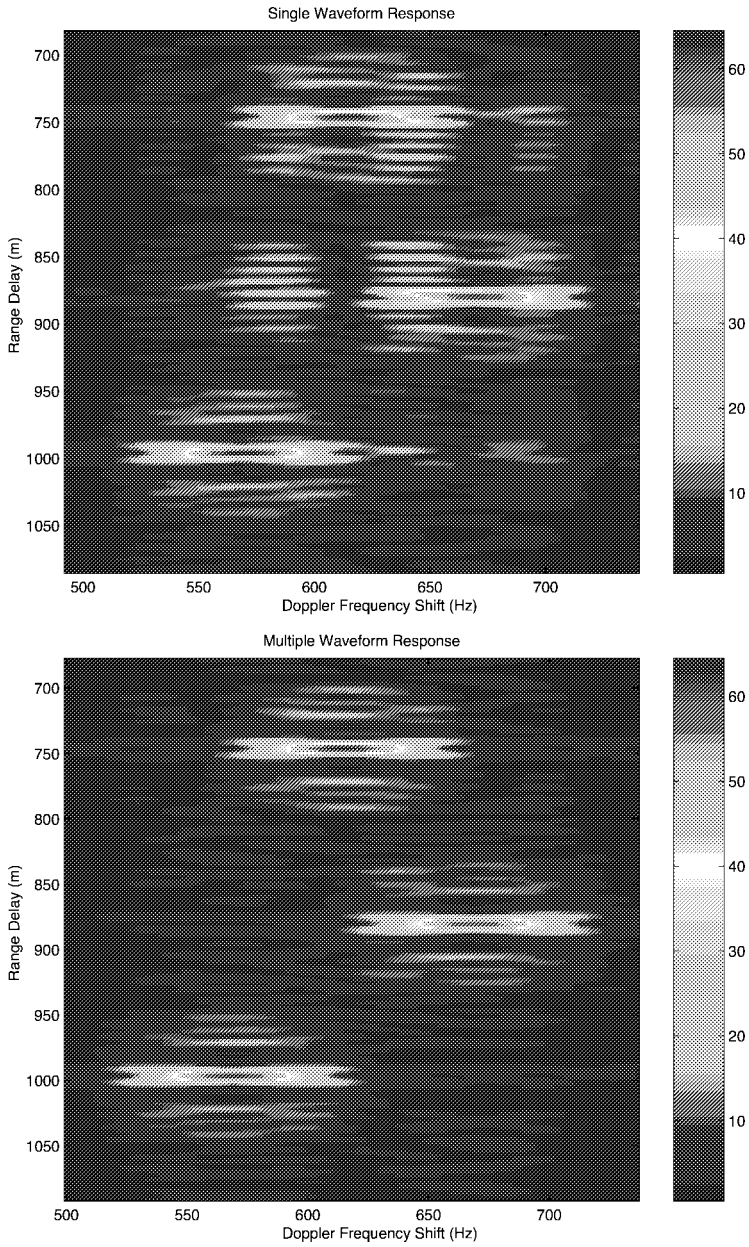


**FIG. 6.** Enlarged delay–Doppler response for three target scenario.

a single waveform pulse train and standard pulse–Doppler processor to make initial surveillance measurements. Then for target clusters where increased discrimination or resolution is required, the radar could switch to making diversity waveform measurements and using the multiplexed–waveform pulse–Doppler processor to achieve enhanced performance. The fact that ghost targets are not present when initial target detection occurs means that false detections resulting from the ghost images need not be dealt with. Once the locations of

targets or target clusters are known, it can be determined whether there will be significant ghost target interference in diversity waveform mode. Processor complexity is another important issue. The standard pulse–Doppler processor implements a bank of linear-time-invariant matched filters (corresponding to the Doppler shifted pulse train). The filter is time-invariant because the pulse matched filter does not change. This leads to a very efficient processor implementation. The multiplexed–waveform pulse–Doppler processor is not time-invariant. The multiplexing of the pulse matched filter destroys the time-invariance and gives rise to a linear time-varying band of (Doppler) filters. Thus synchronization between pulse transmission and signal processing is required. To process all range cells required an increase in processor complexity that is greater than that of the standard pulse–Doppler processor by a factor corresponding to the number of different waveforms in the pulse train, as well as some additional processor complexity to synchronize data flow in the processor. So overall, while this processor is more complex, it is not significantly so.

Finally, we note that this processor is only one form of suboptimal processor for diversity waveform processing. This paper reports work in progress.The development of other processing techniques for diversity waveform processing needs further investigation.

## REFERENCES


1. Helstrom, C. W., *Elements of Signal Detection and Estimation.* Prentice Hall, Englewood Cliffs, NJ, 1995
2. Bell, M. R., Information theory and radar waveform design. *IEEE Trans. Inform. Theory* **39** (1993), 1578–1597.
3. Guey, J. -C. and Bell, M. R., Diversity Waveform sets for delay–Doppler imaging. *IEEE Trans. Inform. Theory* **44** (1998), 1504–1522.
4. Blahut, R. E., Theory of remote surveillance algorithms, In *Radar and Sonar,* Part I (Blahut, R. E., Miller, W., and Wilcox, C. H., Eds.). Springer-Verlag, New York, 1991.
5. Sidiropoulos, N., Baras, J., and Bernstein, C., Two-dimensional signal deconvolution using multiple sensors, In *Proc. Conf. Info. Sciences and Systems.* Johns Hopkins Univ., March 20–22, 1991, pp. 594–599.
6. Komatsu, T., Igarashi, T., Aizawa, K., and Saito, T., Very high resolution imaging scheme with multiple different-aperture cameras. *Signal Process. Image Commun.* **5** (1993), 511–526.
7. Yaroslavsky, L. P. and Caulfield, H. J., Deconvolution of multiple images of the same object, *Appl. Optics* **33** (1994), 2157–2162.
8. Bernfeld, M., Chirp Doppler radar. *Proc. IEEE* **72** (1984), 540–541.
9. Bernfeld, M., Tomography in radar. In *Signal Processing, Part II: Control Theory and Applications* (Grünbaum, F. A., Helton, J. W., and Khargonekar, P., Eds.). Springer-Verlag, New York, 1990.
10. Bell, M. R. and Grubbs, R. A., Modeling and measurement of jet engine modulated radar signal returns for target identification. *IEEE Trans. Aerospace Electron. Systems* **29** (1993), 73–87.
11. Sowelam, S. M. and Tewfik, A. H., Optimal waveforms for wideband radar imaging, *J. Franklin Inst.* **335B** (1998), 1341–1366.
12. Goodman, J. W., *Fourier Optics.* McGraw-Hill, New York, 1968.
13. Woodward, P. M., *Probability and Information Theory, with Applications to Radar.* Pergamon Press, London, 1953.
14. Snyder, D. L. and Whitehouse, H. J., Delay–Doppler radar imaging using chirp-rate modulation. In *Tenth Colloq. GRETSI.* Nice, France, 1985.
15. Snyder, D. L., Whitehouse, H. J., Wohlschlaeger, J. T., and Lewis, R. C., A new approach to radar/sonar imaging. *Proc. SPIE* **10** (1986), 696.

16. Sivaswamy, R., Multiphase complementary codes. *IEEE Trans. Inform. Theory* **24** (1978), 546–552.
17. Sivaswamy, R., Self-clutter cancellation and ambiguity properties of subcomplementary sequences, *IEEE Trans. Aero. Electron. Systems* **18** (1982), 163–181.
18. Hlawatsch, F., *Time Frequency Analysis and Synthesis of Linear Signal Spaces.* Kluwer Academic, Boston, MA, 1998

---

MARK R. BELL received a B.S. in electrical engineering from California State University, Long Beach, in 1981 and the M.S. and Ph.D. in electrical engineering from the California Institute of Technology in 1982 and 1988, respectively. From 1979 to 1989 he was employed by Hughes Aircraft Company, Fullerton, CA. From 1981 to 1989 he was affiliated with the Radar Systems Laboratory at Hughes, where he held the positions of member of the technical staff and staff engineer and worked in the areas of radar signal processing, electromagnetic scattering, radar target identification, and radar systems analysis. While at Caltech, he held a Howard Hughes Doctoral Fellowship from 1984 to 1988. Since 1989, he has been on the faculty of Purdue University, West Lafayette, Indiana, where he is an associate professor in the School of Electrical and Computer Engineering. His research interests are in the areas of radar and sonar, information theory, detection and estimation, and optical communications.

STEPHANE MONROCQ received the B.S. in electrical engineering from CPE Lyon, France, in 2000 and the M.S. in electrical engineering from Purdue University in 2001. Since 2001, he has been employed by Thales Avionics, France and works on Adaptive Antennas for G.P.S. (Global Positioning System) as a research and development engineer in the Department of Navigation Systems—Advanced Studies.